Journal of Materials Chemistry C

PAPER

View Article Online
View Journal | View Issue

Cite this: J. Mater. Chem. C, 2014, 2, 8707

Wet-process feasible novel carbazole-type molecular host for high efficiency phosphorescent organic light emitting diodes†

Jwo-Huei Jou,*[a] Sudhir Kumar,[a] Daiva Tavgeniene,[b] Chih-Chia An,[a] Po-Hsun Fang,[a] Ernestas Zaleckas,[b] Juozas V. Grazulevicius[b] and Saulius Grigalevicius*[b]

Received 2nd July 2014
Accepted 22nd August 2014

DOI: 10.1039/c4tc01423e

www.rsc.org/MaterialsC

Wet-process organic light-emitting diodes (OLEDs) are crucial to realize cost-effective and large-area roll-to-roll fabrication of high quality displays and lightings. In this study, a wet-process feasible carbazole based host material, 2-[4-(carbazol-9-yl)butyloxy]-9-[4-(carbazol-9-yl)butyl]carbazole (**6**), is synthesized, and two other carbazole hosts, 2-[5-(carbazol-9-yl)pentyloxy]-9-[5-(carbazol-9-yl)pentyl]carbazole (**7**) and 2-[6-(carbazol-9-yl)hexyloxy]-9-[6-(carbazol-9-yl)hexyl]carbazole (**8**) are also synthesized for comparison. All the three host materials exhibit high triplet energy, and possess high solubility in common organic solvents at room temperature. On doping a green phosphorescent emitter *fac* tris(2-phenylpyridine)iridium ($Ir(ppy)_3$) into host **6**, the device shows an efficacy of 51 lm W^{-1} and a current efficiency of 52 cd A^{-1} at 100 cd m^{-2} or 30 lm W^{-1} and 40.7 cd A^{-1} at 1000 cd m^{-2}. The high efficiency may be attributed to the host possessing an effective host-to-guest energy transfer, the ability for excitons to generate on both host and guest, and excellent film integrity.

1. Introduction

Organic light emitting diode (OLED) is a potential technology to realize high quality displays and solid state lightings.[1–3] Nowadays, a wide range of OLED based portable display products and some large size displays have already been in the market.[4,5] Recently, phosphorescent OLEDs have drawn considerable attention because of their ability to harvest both singlet and triplet excitons simultaneously through intersystem crossing, approaching near 100% internal quantum efficiency.[6–9] An appropriate molecular host material is required to minimize concentration quenching effects and triplet–triplet annihilation in an undoped phosphorescent emitter[10] A high-triplet energy molecular host material is crucial because it can be used to confine triplet excitons on the emitter and balance carrier injection.[11–14]

OLED devices can be fabricated by the thermal evaporation and spin-coating deposition of organic molecular materials. Thermal evaporation appears to be a successful approach to achieve high efficiency with small molecular hosts. However, it is limited due to numerous issues such as condition of high thermal stability of organic molecules, low throughput and comparatively higher cost due to the huge wastage of organic materials in the chamber itself. To make the resultant products highly cost-effective and large-area roll-to-roll fabrication, solution-processable OLEDs with higher efficiencies are in extreme demand.[15–19]

Over the past years, compared with vapor-deposited counterparts,[20–23] wet-process feasible molecular hosts for phosphorescent OLEDs have rarely been reported.[12, 24–32] Kakimoto and co-workers reported a maximum efficacy of 4.4 lm W^{-1} by doping an $Ir(ppy)_3$ guest into triphenylamine/benzimidazole hybrid as host, tris(2-methyl-3′-(1-phenyl-1*H*-benzimidazol-2-yl)biphenyl-4-yl)amine.[31] A maximum efficacy of 7.3 lm W^{-1} was realized by doping a bipolar host, tris(2,2′-dimethyl-4′-(1-phenyl-1*H*-benzimidazol-2-yl)biphenyl-4-yl)amine with $Ir(ppy)_3$ guest.[32] Kido and co-workers reported an efficacy of 11 lm W^{-1} at 100 cd m^{-2} by employing a carbazole-type host, 1,3-bis(3-(3,6-di-*n*-butylcarbazol-9-yl) phenyl)benzene, and tris(2-(4-tolyl)phenylpyridine)iridium(III) as guest.[33] Jou and Grigalevicius's groups reported bipolar carbazole/phenylindole hybrid as host, 9,9′-bis[6-(carbazol-9-yl)hexyl][3,3′]bicarbazole, and an efficacy of 16.4 lm W^{-1} was realized by using $Ir(ppy)_3$ as guest.[34] Ma and Yang's groups achieved an efficacy of 26 lm W^{-1} by using a oxadiazole/triphenylamine hybrid, 2-(3,5-bis(4′-(diphenylamino)phenyl) phenyl)-5-(4-*tert*-butylphenyl)-1,3,4-oxadiazole, as host.[35] Hence, synthesizing a wet-process feasible molecular host is greatly considerable to realize low cost, large-area, high throughput and high performance OLED based products.

[a]*Department of Materials Science and Engineering, National Tsing-Hua University, Hsin-Chu-30013, Taiwan, Republic Of China. E-mail: jjou@mx.nthu.edu.tw*

[b]*Department of Polymer Chemistry and Technology, Kaunas University of Technology, Radvilenu plentas 19, LT50254, Kaunas, Lithuania. E-mail: saulius.grigalevicius@ktu.lt*

† Electronic supplementary information (ESI) available. See DOI: 10.1039/c4tc01423e

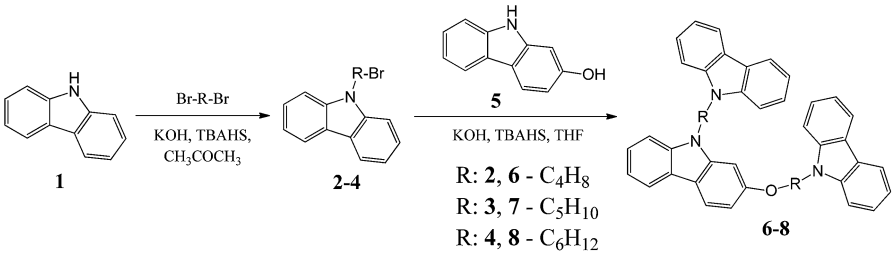

Scheme 1 Schematic illustration of the synthesis of the carbazole-type hosts, **6**, **7**, and **8**.

Table 1 Photophysical and electrochemical characteristics of the novel host **6**, compared with those of the small molecular hosts **7** and **8**

Host	λ_{ab} [nm]	λ_{em} [nm]	E_T[a] [eV]	E_S[b] [eV]	HOMO[c] [eV]	LUMO[d] [eV]	T_g[e] [°C]	T_d[f] [°C]
6	345	356, 368	2.95	3.54	5.48	1.95	64	361
7	345	368	2.95	3.54	5.48	1.95	58	345
8	345	369	2.96	3.52	5.47	1.96	20	338

[a] Triplet-energy level at 77 K. [b] Singlet energy-gap. [c] HOMO values are measured by the cyclic voltammetry (CV) method. The semi-oxidation potential ($E^{ox}_{1/2}$) could be calculated from $(E_{p1} + E_{p2})/2 - 0.48$, where 0.48 is the correction value obtained by the oxidation system added to ferrocenium/ferrocene (Fc^+/Fc) as the internal standard, and then the energy of HOMO could be obtained from the $E_{HOMO} = -(E^{ox}_{1/2} + 4.8)$. [d] The energy of LUMO could be obtained by subtracting the optical bandgap from the HOMO energy level, $[E_{LUMO} = (E_{HOMO} - E_g)]$. [e] Glass transition temperature. [f] Thermal decomposition temperature.

In this study, a high-efficiency, green phosphorescent OLED fabricated by employing a wet-process feasible newly synthesized carbazole-type host material, 2-[4-(carbazol-9-yl)butyloxy]-9-[4-(carbazol-9-yl)butyl]carbazole (**6**) that possesses high triplet-energy and low carrier injection barrier is presented. In the device doped with $Ir(ppy)_3$ guest, the host **6** exhibits a power efficiency of 51 lm W^{-1} and a current efficiency of 52 cd A^{-2} at 100 cd m^{-2}. For comparison, two other hosts, 2-[5-(carbazol-9-yl)pentyloxy]-9-[5-(carbazol-9-yl)pentyl]carbazole (**7**) and 2-[6-(carbazol-9-yl)hexyloxy]-9-[6-(carbazol-9-yl)hexyl]carbazole (**8**), were also studied. For host **7** containing device, its power efficiency was 29.1 lm W^{-1} (37.5 cd A^{-1}), while 23.3 lm W^{-1} (35.9 cd A^{-1}) for the compound **8**-containing counterpart.

2. Result and discussion

2.1 Synthesis of the host materials

Carbazole-type host materials, 2-[4-(carbazol-9-yl)butyloxy]-9-[4-(carbazol-9-yl)buty]carbazole (**6**), 2-[5-(carbazol-9-yl)pentyloxy]-9-[5-(carbazol-9-yl)pentyl]carbazole (**7**) and 2-[6-(carbazol-9-yl) hexyloxy]-9-[6-(carbazol-9-yl)hexyl]carbazole (**8**), were synthesized using rather simple alkylation methods, as shown in Scheme 1. The key starting materials, 9-(bromoalkyl)carbazoles (**2–4**) were prepared from commercially available 9*H*-carbazole (**1**) and an excess of corresponding dibromoalkane under basic conditions using tetra-*n*-butyl ammonium hydrogen sulphate (TBAHS) as a phase transfer catalyst. The compounds **2–4** were

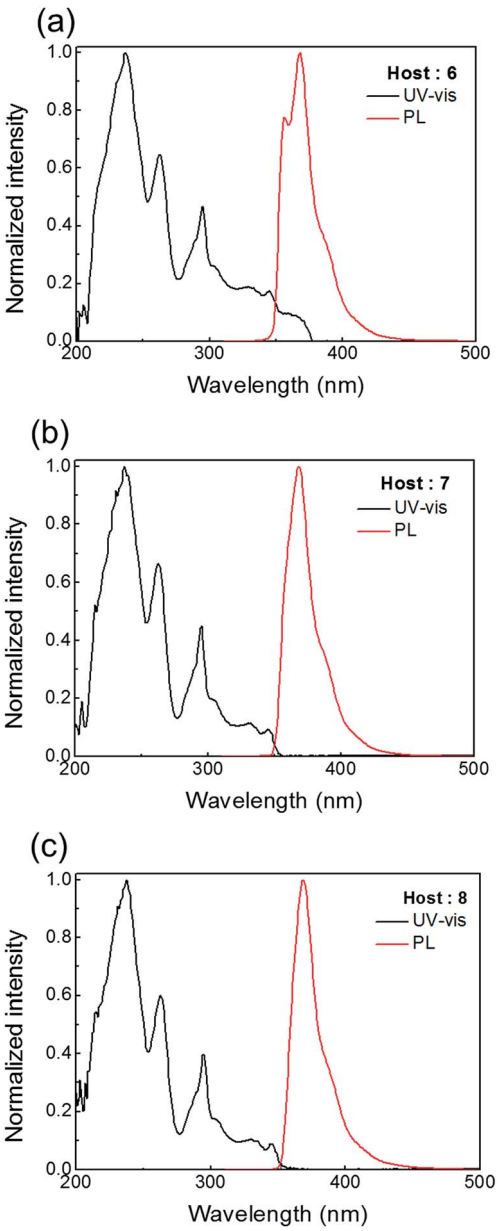

Fig. 1 Ultraviolet-visible and photoluminescence spectra of the novel carbazole-type host materials, (a) **6**, (b) **7**, and (c) **8**. All the data were measured in tetrahydrofuran at room temperature.

reacted with 2-hydroxycarbazole (**5**) under basic conditions to afford the carbazolyl containing derivatives **6–8** as host materials. The newly synthesized derivatives were confirmed by ^{1}H NMR spectroscopy and mass spectrometry (ESI Fig. S1–S3†). The data were found to be in good agreement with the proposed structures. The derivatives were soluble in common organic solvents such as acetone, chloroform or THF at room temperature.

2.2 Photophysical and electrochemical characteristics

Table 1 shows the photophysical properties of the three carbazole based host materials. Fig. 1 shows the ultraviolet-visible (UV-vis) and photoluminescence (PL) spectra of the materials **6–8** dissolved in tetrahydrofuran (THF) at room temperature. The singlet energy gaps were calculated from the intersection of UV-vis absorption peaks, giving values of 3.54, 3.54 and 3.52 eV for compounds **6**, **7** and **8**, respectively.

The experimentally determined triplet-energies were 2.95 eV, 2.95 eV, and 2.96 eV for the materials **6**, **7** and **8**, respectively, which were calculated from the first phosphorescent emission peak of low temperature (77 K) PL spectra at 420 nm, 420 nm and 419 nm, respectively, as shown in Fig. 2(a). These results show that the triplet-energies of these three host materials are extensively higher than that of the green emitter, Ir(ppy)$_3$, which exhibited a triplet-energy value of the 2.57 eV.[36,37] These host materials should enable the occurrence of effective energy transfer from host-to-guest and exciton confinement on guest, resulting in good device efficiency.[12, 38–40] Hence, these values of triplet energies are sufficiently higher to effectively confine the triplet excitons on the guest and extensively prohibit back energy transfer to the hosts. Both photophysical and electrochemical properties of all the three hosts remain almost unchanged by increasing the length of alkyl and alkyl ether linkages.

The electrochemical properties of the three carbazole-type host molecules **6–8** were measured by cyclic voltammetry (ESI Fig. S4†). The highest occupied molecular orbital (HOMO) energy levels were estimated to be 5.48 eV, 5.48 eV, and 5.47 eV for **6**, **7**, and **8**, respectively, using oxidation potential. The lowest unoccupied molecular orbital (LUMO) energy levels of the emitters were calculated to be 1.95 eV, 1.95 eV, and 1.96 eV for **6**, **7**, and **8**, respectively, from HOMO energy levels and

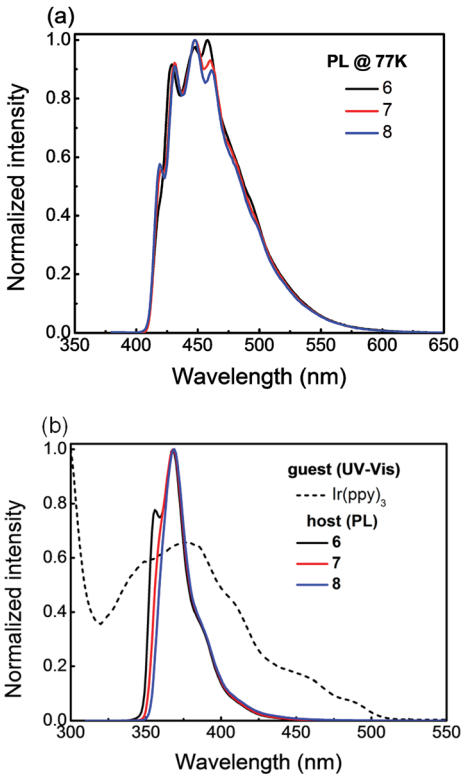

Fig. 2 Photoluminescence (PL) spectra of the newly synthesized hosts **6**, **7**, and **8** measured in tetrahydrofuran (a) at 77 K and (b) at room temperature. The ultraviolet-visible (UV-vis) spectrum of the green Ir(ppy)$_3$ guest molecule is also shown. The comparatively large overlapping area between the **6** host PL and the green emitter UV-vis spectra indicates a higher efficient host to guest energy transfer occurring in the **6**-containing green OLED.

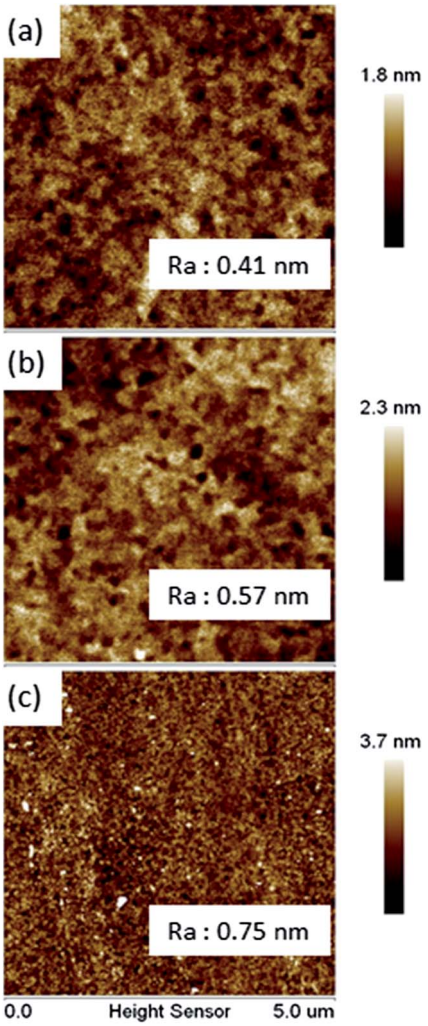

Fig. 3 Surface morphologies of the spin-coated films that comprise the pure hosts (a) **6**, (b) **7**, and (c) **8**. All the films uniformities are improved upon increasing the glass transition temperature (T_g).

optical energy band gaps, which were estimated from the intersection of absorption and emission spectra (Table 1).

2.3 Thermal and morphological characteristics

As measured using differential scanning calorimetry (DSC), the host molecule **6** showed a glass transition temperature (T_g) of 64 °C, 58 °C for **7** and 20 °C for **8** (Table 1). The slightly higher T_g of the host **6** indicated a strong intermolecular interaction of carbazole units due to short chain alkyl ether and alkyl junctions. As investigated using thermogravimetric analysis (TGA), the host **6** exhibited a thermal decomposition temperature (T_d) of 361 °C, corresponding to a 5% weight loss, while 345 °C for **7** and 338 °C for **8**. The higher T_g and T_d characteristic of the host **6** facilitated relatively better film integrity during the entire fabrication process, especially during solvent removal.[41,42]

Fig. 3 shows the atomic-force microscopy (AFM) images of the compounds, **6**, **7**, and **8** containing films by spin-coating. The respective surface roughness values are 0.41, 0.57 and 0.75 nm, while the corresponding glass transition temperatures (T_g) are 65, 58 and 20 °C. The surface roughness became smoother as the T_g of the host material was increased. The relatively better film integrity may explain why compound **7** containing devices

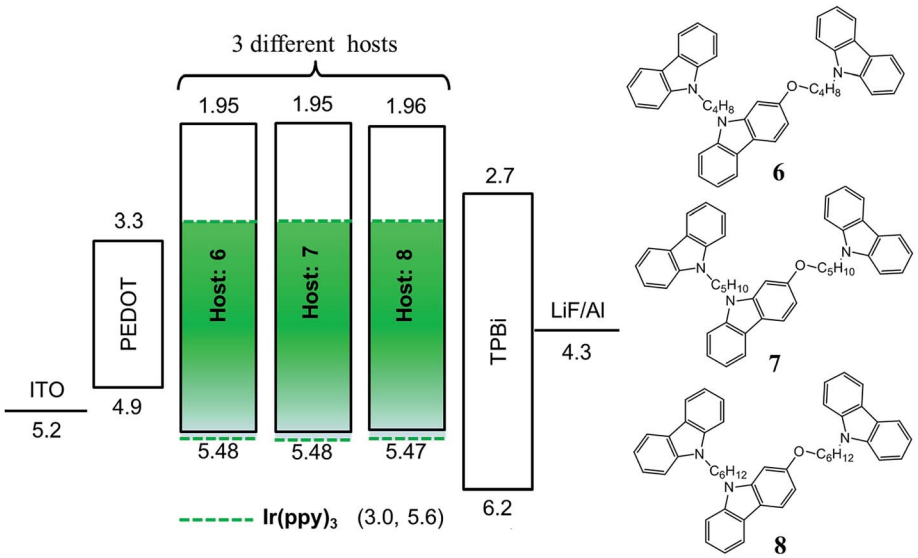

Fig. 4 Schematic diagram of the energy-levels of the OLED device containing the presented host materials, **6**, **7**, and **8**. Molecular structures of the three studied hosts are also shown.

Table 2 Effects of the different doping concentrations of $Ir(ppy)_3$ on the operation voltage (OV), power efficiency (η_p), current efficiency (η_c), external quantum efficiency (η_{ext}) and CIE coordinates of the novel host materials **6**, **7**, and **8**-containing OLED devices

Host	Wt% ratio of dopant	@ 100/1000 cd m^{-2} OV [V]	η_p [lm W^{-1}]	η_c [cd A^{-1}]	η_{ext} [%]	1931 CIE coordinates	Maximum luminance [cd m^{-2}]
6	5	4.7/6.0	22.7/14.1	34.0/26.7	9.5/7.4	(0.29, 0.63)/(0.29, 0.63)	7899
	10	4.0/5.2	33.8/21.5	43.3/35.2	11.6/9.5	(0.30, 0.63)/(0.30, 0.63)	11 010
	15	3.6/4.7	36.3/23.2	41.8/34.5	11.5/9.5	(0.32, 0.62)/(0.32, 0.62)	13 800
	20	3.5/4.5	44.6/26.9	49.8/38.7	13.6/10.6	(0.31, 0.63)/(0.31, 0.63)	11 250
	25	3.2/4.3	50.8/30.3	51.8/40.7	14.1/11.1	(0.31, 0.63)/(0.31, 0.63)	12 600
	30	3.0/3.9	37.9/28.3	36.7/34.5	10.1/9.5	(0.33, 0.62)/(0.32, 0.62)	14 510
7	5	6.9/8.5	25.4/14.3	55.6/38.8	7.5/6.0	(0.30, 0.63)/(0.30, 0.63)	5761
	10	6.4/8.1	27.7/16.2	56.3/41.8	7.8/6.5	(0.31, 0.63)/(0.31, 0.63)	8447
	15	4.0/5.5	32.1/18.5	40.8/32.4	10.6/7.3	(0.32, 0.62)/(0.32, 0.62)	8954
	20	3.7/4.9	39.5/24.2	46.7/38.1	12.0/9.2	(0.32, 0.62)/(0.32, 0.62)	12 750
	25	3.4/4.4	38.0/25.2	40.8/35.1	12.2/9.6	(0.33, 0.62)/(0.33, 0.62)	15 730
	30	3.1/4.1	42.5/29.1	42.2/37.5	9.9/8.6	(0.33, 0.62)/(0.33, 0.62)	17 810
8	5	3.5/4.6	25.2/15.9	28.4/23.1	15.1/10.3	(0.30, 0.63)/(0.30, 0.63)	6391
	10	4.6/6.0	22.3/13.0	32.4/25.1	14.8/11.3	(0.30, 0.63)/(0.30, 0.63)	7767
	15	4.3/5.6	31.1/16.2	41.9/28.8	10.6/8.9	(0.30, 0.63)/(0.30, 0.63)	9028
	20	3.8/4.9	38.1/23.3	46.0/35.9	13/10.4	(0.31, 0.63)/(0.31, 0.63)	10 830
	30	3.5/5.1	39.0/21.4	43.9/34.6	11.3/9.8	(0.33, 0.62)/(0.32, 0.62)	9252
	35	3.7/5.3	30.4/18.7	36.1/31.1	10.6/10.1	(0.32, 0.62)/(0.32, 0.62)	7194

showed better efficiency than the compound **8** containing counterpart.

2.4 Electroluminescent characteristics of devices

Fig. 4 illustrates the schematic energy-level diagram of green OLED devices and the molecular structures of the newly synthesized host materials, **6**, **7**, and **8**. The devices are composed of a 125 nm indium tin oxide (ITO) anode layer, a 35 nm poly(3,4-ethylene-dioxythiophene)-poly(styrenesulfonate) (PEDOT:PSS) hole injection layer (HIL), a 20 nm single emissive layer (EML) with the $Ir(ppy)_3$ emitter doped in compound **6** host *via* spin-coating, a 32 nm 1,3,5-tris(*N*-phenyl-benzimidazol-2-yl) benzene (TPBi) electron transporting layer (ETL), a 1 nm lithium fluoride (LiF) layer, and a 100 nm aluminum (Al) cathode layer. In addition, the host **6**, two other compounds, **7** and **8**, were also studied for comparison.

Table 2 shows the electroluminescent characteristics of the host **6** containing green OLED compared with that of the **7** and **8**-containing counterparts. As shown in Fig. 5, host **6** containing device exhibited a power efficiency of 30.3 lm W^{-1} with a current efficiency of 40.7 cd A^{-1} at 1000 cd m^{-2}, which is the highest among all the three host containing devices. For host **7** containing device, its power efficiency was 29.1 lm W^{-1} (37.5 cd A^{-1}), while 23.3 lm W^{-1} (35.9 cd A^{-1}) for the host **8** containing counterpart.

As illustrated in Fig. 4, the architectures of the three hosts, **6**, **7**, and **8**, containing device significantly favors the injection of holes to the hosts because they exhibit a hole injection barrier of around 0.58 eV, which is 0.12 eV lower than that of the hole to the guest (0.7 eV). While, the same architectures favor the injection of electron into the $Ir(ppy)_3$ guest because there exists a −0.2 eV electron trap, while there is an around 0.75 eV barrier for electron to enter into the hosts. Hence, these would lead excitons to generate on both host and guest and result in high device efficiency.[19]

Compound **6** containing device showed a highest efficiency. EL properties, including power efficiency, current efficiency and EQE, were different for the devices containing the three compounds **6**, **7** and **8** because of the difference in the effectiveness of host-to-guest energy transfer. As shown in Fig. 2(b), the overlapping area between the absorption spectrum of guest (UV-vis of $Ir(ppy)_3$) and the emission spectrum of host (PL) was the largest for compound **6**, indicating a comparatively higher host-to-guest energy transfer. Furthermore, compound **6** showed an additional emission peaking at the lower wavelength site (356 nm), which would trigger the higher energy emission of the guest. This explains why the resultant electroluminescent (EL) spectrum of the green $Ir(ppy)_3$ doped into compound **6** was blue-shifted as compared with those into compounds **7** and **8** as host, as shown in Fig. 6. There is only guest, $Ir(ppy)_3$, emission without any emission from hosts. This shows that the energy was effectively transferred from the host to the guest.

As shown in Fig. 7, the device efficiency extensively depends on the doping concentration of the green emitter. Taking the host **6**-based device for example, the power efficiency at 1000 cd m^{-2} increased from 14.1 to 30.3 lm W^{-1} as doping

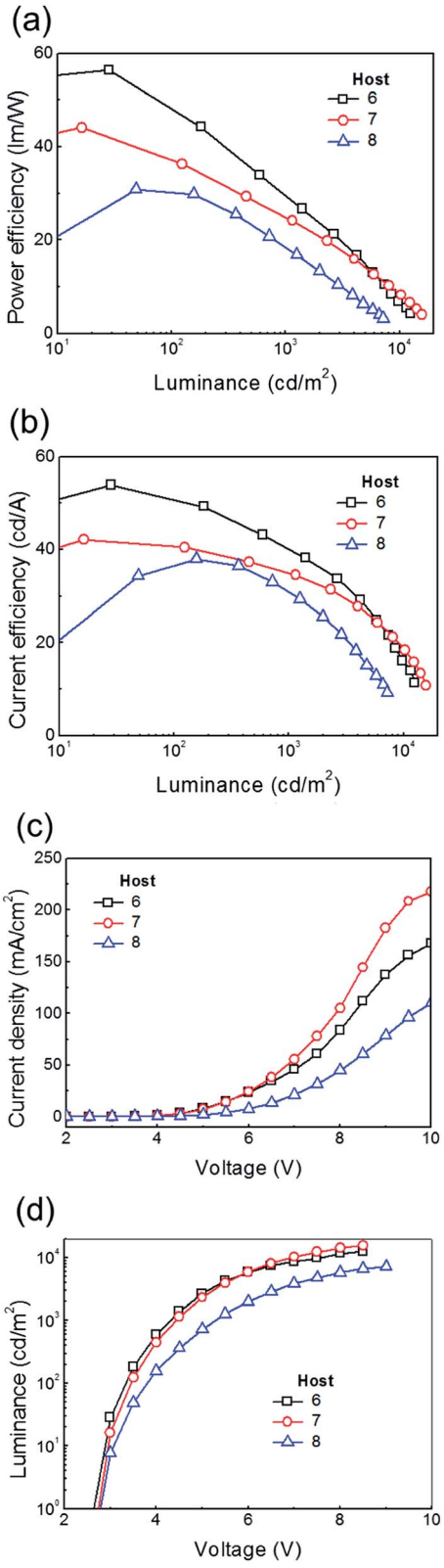

Fig. 5 Comparison of (a) power efficiency, (b) current efficiency, (c) current density, and (d) luminance of the devices with the 25 wt% ratio $Ir(ppy)_3$ doped in the host materials, **6**, **7** and **8**.

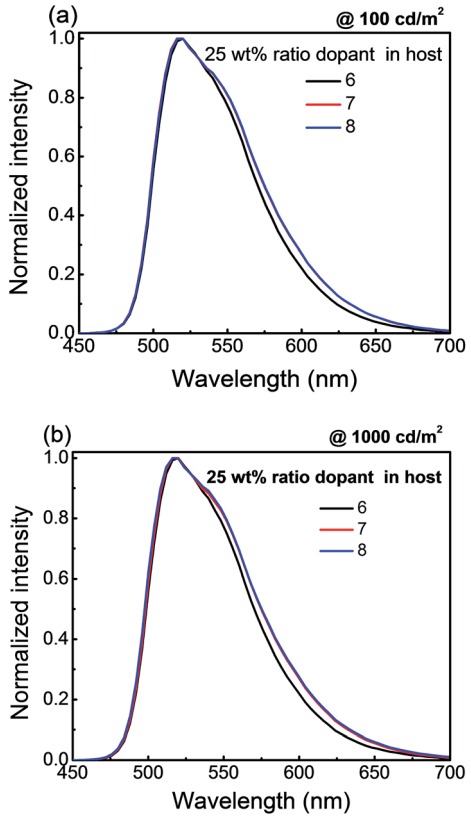

Fig. 6 Host effect on the electroluminescence (EL) spectra of the devices containing three different host molecules, **6**, **7** and **8**, with 25 wt% ratio green emitter, $Ir(ppy)_3$. The EL emission spectrum becomes slightly broader as the host material is changed from **6** to **7** or **8**, while the spectra remain unchanged even at a higher luminance, 1000 cd m^{-2}.

concentration was increased from 5 to 25 wt%. The resulting device showed the highest efficiency among all the studied concentrations as 25 wt% guest was doped into the host **6**. However, as the concentration increased to 30 wt%, the power efficiency started to decrease. This may be attributed to the concentration-quenching efficiency roll-off, resulting from the self-segregation of the emitter at high concentrations.

When material **8** was employed as the host, the resultant device exhibited a power efficiency of 15.9 lm W^{-1} (23.1 cd A^{-1}) at 1000 cd m^{-2} with a 5 wt% doping concentration of $Ir(ppy)_3$ guest. The efficiency becomes higher as the dopant concentration increased from 5 to 20 wt%. At 20 wt%, for example, the power efficiency is 23.3 lm W^{-1} (35.9 cd A^{-1}). As the dopant concentration increased further to 35 wt%, the efficacy reduces to 18.7 lm W^{-1} (31.1 cd A^{-1}). Host **7** containing device showed the best efficacy of 29.1 lm W^{-1} (35.9 cd A^{-1}) with a 30 wt% doping concentration of $Ir(ppy)_3$. Compared to that of the counterpart **8**, the higher efficiency exhibited by the host **7** containing device may result mainly from the fact that material **8** showed a poor film integrity due to much lower T_g of 20 °C.

Furthermore, we investigated the effect of all the three hosts, **6**, **7** and **8** devices operational stability, t_{50}, based on solution-process feasible emissive layer. The operational lifetime of all the devices was investigated without encapsulation. As

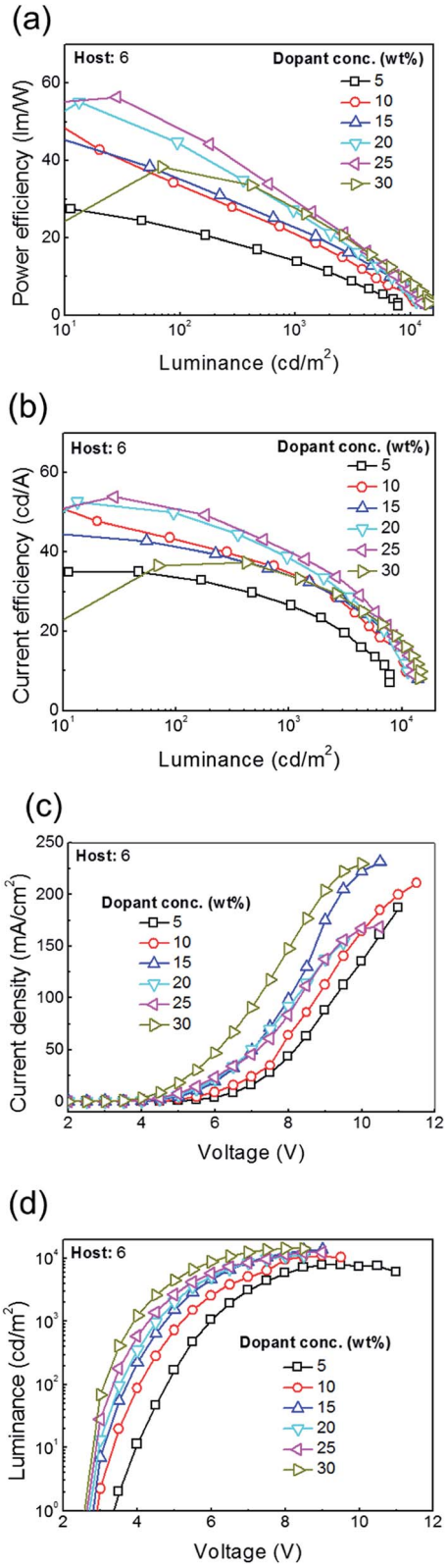

Fig. 7 Doping concentration (weight ratio with host) effects on the (a) power efficiency, (b) current efficiency, (c) current density, and (d) luminance results of the **6** host based green OLED device.

measured at an initial brightness of 800 cd m^{-2}, the resultant devices have shown the operational stability of 27, 12 and 5.4 min, respectively, for compounds **6**, **7** and **8** (ESI Fig. S5†).

3. Conclusion

To conclude, in this report we demonstrated a molecular carbazole-based host **6** with wet-process feasibility. By employing this host, green phosphorescent OLED devices with higher efficiencies have been fabricated. The resulting device shows at 100 cd m^{-2}, for example, a power efficiency of 51 lm W^{-1} and a current efficiency of 52 cd A^{-1} for a simple double layer green phosphorescent OLED device. High efficiency may be attributed to the host possessing an effective host-to-guest energy transfer. The facile synthesis, excellent solubility in common organic solvents, excellent film integrity and very high triplet energy come together to ensure that compound **6** can be a promising host material for the low cost and large-area roll-to-roll fabrication of energy-efficient phosphorescent OLEDs.

4. Experimental methods

4.1 Materials characteristics and measurements

All the precursor compounds required for the synthesis were purchased from commercial sources and used without any purification. Column chromatography purifications were performed with silica gel (70–230 mesh) as a stationary phase in a column 50 cm long and 5 cm in diameter. ^{1}H NMR spectra were recorded using a Varian Unity Inova (300 MHz) apparatus. Mass spectra of the compounds were obtained on a Waters ZQ 2000 spectrometer in the positive ion mode. EL spectra were recorded in tetrahydrofuran at room temperature in quartz cuvettes using a Fluorolog III photoluminescence spectrometer. UV-vis spectra were recorded in toluene at room temperature using a UV-vis spectrophotometer.

Cyclic voltammetry (CV) experiments were performed on an electrochemical workstation using a three electrode assembly comprising glassy carbon working electrode, a non-aqueous Ag/AgCl reference electrode and an auxiliary platinum electrode. The experiments were performed at room temperature under nitrogen atmosphere in dichloromethane using 0.1 M tetrabutylammonium perchlorate (Bu_4NClO_4) as supporting electrolyte on a Chinstruments CH1604A potentiostat. The $E^{ox}_{1/2}$ values were determined as $(E^a_p + E^c_p)/2$, where E^a_p and E^c_p are the anodic and cathodic peak potentials, respectively. Differential scanning calorimetry (DSC) measurements were carried out using a Bruker Reflex II thermosystem. The DSC curves were recorded in a nitrogen atmosphere at a heating rate of 10 °C min^{-1}. Thermogravimetric analysis (TGA) was performed under a continuous nitrogen flow using a TGA Q50 apparatus at a heating rate of 10 °C min^{-1}.

4.2 Device fabrication and characterization

Fig. 4 shows the schematic energy-level diagram of green OLEDs studied here. The fabrication process included first spin-coating an aqueous solution of PEDOT:PSS at 4000 rpm for 20 s to form a hole-injection layer (HIL) on a pre-cleaned ITO anode. Before depositing the following emissive layer, the solution was prepared by dissolving the $Ir(ppy)_3$ guest in three different novel host molecules, **6**, **7** and **8**, in tetrahydrofuran at room-temperature for 0.5 h with stirring. The resulting solution was then spin-coated at 2500 rpm for 20 s under nitrogen. Thereafter, the electron-transporting layer TPBi, the electron injection layer LiF, and the cathode Al, were deposited by thermal evaporation in a vacuum chamber at the vacuum level of less than 5×10^{-6} Torr.

The luminance, CIE chromatic coordinates, and electroluminescent spectrum of the resultant green OLEDs were measured by using Photo Research PR-655 spectrascan. Keithley 2400 electrometer was used to measure the current–voltage (*I–V*) characteristics. The emission area of the devices was 25 mm^2, and only the luminance in the forward direction was measured.

Acknowledgements

This work was financially supported by National Science Council through the grant numbers of 100-2119-M-007-011-MY3 and 103-2923-E-007-003-MY3, Ministry of Economic Affairs through the grant number MEA 102-EC-17-A-07-S1-181 and by Research Council of Lithuania (project TAPLLT1/14).

References

1 F. So, J. Kido and P. Burrows, *MRS Bull.*, 2008, **33**, 663.
2 B. W. D'Andrade and S. R. Forrest, *Adv. Mater.*, 2004, **16**, 1585.
3 M. C. Gather, A. Kohnen and K. Meerholz, *Adv. Mater.*, 2011, **23**, 233.
4 S. R. Forrest, *Nature*, 2004, **428**, 911.
5 S. Reineke, F. Lindner, G. Schwartz, N. Seidler, K. Walzer, B. Lussem and K. Leo, *Nature*, 2009, **459**, 234.
6 M. A. Baldo, D. F. O'Brien, Y. You, A. Shoustikov, S. Sibley, M. E. Thompson and S. R. Forrest, *Nature*, 1998, **395**, 151.
7 C. Adachi, M. A. Baldo and S. R. Forrest, *Appl. Phys. Lett.*, 2000, **77**, 904.
8 J. P. Duan, P. P. Sun and C. H. Cheng, *Adv. Mater.*, 2003, **15**, 224.
9 Q. Zhang, Q. Zhou, Y. Cheng, L. Wang, D. Ma and X. Jing, *Adv. Mater.*, 2004, **16**, 432.
10 S.-J. Yeh, M.-F. Wu, C.-T. Chen, Y.-H. Song, Y. Chi, M.-H. Ho, S.-F. Hsu and C.-H. Chen, *Adv. Mater.*, 2005, **17**, 285.
11 R. J. Holmes, S. R. Forrest, Y.-J. Tung, R. C. Kwong, J. J. Brown, S. Garon and M. E. Thompson, *Appl. Phys. Lett.*, 2003, **82**, 2422.
12 S. Tokito, T. Iijima, Y. Suzuri, H. Kita, T. Tsuzuki and F. Sato, *Appl. Phys. Lett.*, 2003, **83**, 569.
13 S.-J. Su, H. Sasabe, T. Takeda and J. Kido, *Chem. Mater.*, 2008, **20**, 1691.
14 S.-J. Su, C. Cai and J. Kido, *Chem. Mater.*, 2011, **23**, 274.
15 J. S. Chen, C. S. Shi, Q. Fu, F. C. Zhao, Y. Hu, Y. L. Feng and D. G. Ma, *J. Mater. Chem.*, 2012, **22**, 5164.

16 T.-W. Lee, T. Noh, H.-W. Shin, O. Kwon, J.-J. Park, B.-K. Choi, M.-S. Kim, D. W. Shin and Y.-R. Kim, *Adv. Mater.*, 2009, **19**, 1625.
17 J.-H. Jou, M.-F. Hsu, W.-B. Wang, C.-L. Chin, Y.-C. Chung, C.-T. Chen, J.-J. Shyue, S.-M. Shen, M.-H. Wu, W.-C. Chang, C.-P. Liu, S.-Z. Chen and H.-Y. Chen, *Chem. Mater.*, 2009, **21**, 2565.
18 J.-H. Jou, C.-J. Li, S.-M. Shen, S.-H. Peng, Y.-L. Chen, Y.-C. Jou, J. H. Hong, C.-L. Chin, J.-J. Shyue, S.-P. Chen, J.-Y. Li, P.-H. Wang and C.-C. Chen, *J. Mater. Chem. C*, 2013, **1**, 4201.
19 J.-H. Jou, Y.-M. Yang, S.-Z. Chen, J.-R. Tseng, S.-H. Peng, C.-Y. Hsieh, Y.-X. Lin, C.-L. Chin, J.-J. Shyue, S.-S. Sun, C.-T. Chen, C.-W. Wang, C.-C. Chen, S.-H. Lai and F.-C. Tung, *Adv. Opt. Mater.*, 2013, **1**, 657.
20 F.-M. Hsu, C.-H. Chien, P.-I. Shih and C.-F. Shu, *Chem. Mater.*, 2009, **21**, 1017.
21 Z.-Q. Gao, M. Luo, X.-H. Sun, H.-L. Tam, M.-S. Wong, B.-X. Mi, P.-F. Xia, K.-W. Cheah and C.-H. Chen, *Adv. Mater*, 2009, **21**, 688.
22 T. Zhang, Y. Liang, J. Cheng and J. Li, *J. Mater. Chem. C*, 2013, **1**, 757.
23 H. Sasabe, T. Chiba, S.-J. Su, Y.-J. Pu, K. Nakayama and J. Kido, *Chem. Commun.*, 2008, 5821.
24 L. Duan, L. Hou, T.-W. Lee, J. Qiao, D. Zhang, G. Dong, L. Wang and Y. Qiu, *J. Mater. Chem.*, 2010, **20**, 6392.
25 L. Zeng, T. Y.-H. Lee, P. B. Merkel and S. H. Chen, *J. Mater. Chem.*, 2009, **19**, 8772.
26 B. W. D'Andrade, M. A. Baldo, C. Adachi, J. Brooks, M. E. Thompson and S. R. Forrest, *Appl. Phys. Lett.*, 2001, **79**, 1045.
27 C. Adachi, M. A. Baldo, M. E. Thompson and S. R. Forrest, *J. Appl. Phys.*, 2001, **90**, 5048.
28 M. Ikaia, S. Tokito, Y. Sakamoto, T. Suzuki and Y. Taga, *Appl. Phys. Lett.*, 2001, **79**, 156.
29 Y. Qian, F. Cao and W. Guo, *Tetrahedron*, 2013, **69**, 4169.
30 P. I. Shih, C. L. Chiang, A. K. Dixit, C. K. Chen, M. C. Yuan, R. Y. Lee, C. T. Chen, E. W. G. Diau and C. F. Shu, *Org. Lett.*, 2006, **8**, 2799.
31 Z. Ge, T. Hayakawa, S. Ando, M. Ueda, T. Akiike, H. Miyamoto, T. Kajita and M. Kakimoto, *Chem. Mater.*, 2008, **20**, 2532.
32 Z. Ge, T. Hayakawa, S. Ando, M. Ueda, T. Akiike, H. Miyamoto, T. Kajita and M. Kakimoto, *Adv. Funct. Mater.*, 2008, **18**, 584.
33 N. Aizawa, Y.-J. Pu, H. Sasabe and J. Kido, *Org. Electron.*, 2012, **13**, 2235.
34 D. Mazetyte, G. Krucaite, J. Grazulevicius, C.-I. Chiang, F.-C. Yang, J.-H. Jou and S. Grigalevicius, *Opt. Mater.*, 2013, **35**, 604.
35 M. Zhu, T. Ye, X. He, X. Cao, C. Zhong, D. Ma, J. Qin and C. Yang, *J. Mater. Chem.*, 2011, **21**, 9326.
36 N. Li, S.-L. Lai, W. Liu, P. Wang, J. You, C.-S. Lee and Z. Liu, *J. Mater. Chem.*, 2011, **21**, 12977.
37 X. Yang, D. Neher, D. Hertel and T. K. Däubler, *Adv. Mater.*, 2004, **16**, 161–166.
38 A. P. Kulkarni, C. J. Tonzola, A. Babel and S. A. Jenekhe, *Chem. Mater.*, 2004, **16**, 4556; G. Hughes and M. R. Bryce, *J. Mater. Chem.*, 2005, **15**, 94.
39 Y. Kawamura, S. Yanagida and S. R. Forrest, *J. Appl. Phys.*, 2002, **92**, 87.
40 P. A. Vecchi, A. B. Padmaperuma, H. Qiao, L. S. Sapochak and P. E. Burrows, *Org. Lett.*, 2006, **8**, 4211.
41 J.-H. Jou, W.-B. Wang, S.-Z. Chen, J.-J. Shyue, M.-F. Hsu, C.-W. Lin, S.-M. Shen, C.-J. Wang, C.-P. Liu, C.-T. Chen, M.-F. Wu and S.-W. Liu, *J. Mater. Chem.*, 2010, **20**, 8411.
42 J.-H. Jou, W.-B. Wang, S.-M. Shen, S. Kumar, I.-M. Lai, J.-J. Shyue, S. Lengvinaite, R. Zostautiene, J. V. Grazulevicius, S. Grigalevicius, S.-Z. Chen and C.-C. Wu, *J. Mater. Chem.*, 2011, **21**, 9546.

